JOURNAL OF SCIENCE
SAKARYA UNIVERSITY

Sakarya University Journal of Science

ISSN 1301-4048 | e-ISSN 2147-835X | Period Bimonthly | Founded: 1997 | Publisher Sakarya University | http://www.saujs.sakarya.edu.tr/en/

Title: Modelling of Remazol Black-B Adsorption on Chemically Modified Waste Orange Peel: pH Shifting Effect of Acidic Treatment

Authors: Ceren KARAMAN, Zümriye AKSU
Recieved: 2020-06-11 15:51:04

Accepted: 2020-08-26 17:36:56

Article Type: Research Article
Volume: 24
Issue: 5
Month: October
Year: 2020
Pages: 1135-1150

How to cite
Ceren KARAMAN, Zümriye AKSU; (2020), Modelling of Remazol Black-B Adsorption on Chemically Modified Waste Orange Peel: pH Shifting Effect of Acidic Treatment. Sakarya University Journal of Science, 24(5), 1135-1150, DOI: https://doi.org/10.16984/saufenbilder.751491
Access link
http://www.saujs.sakarya.edu.tr/en/pub/issue/56422/751491

Sakarya University Journal of Science 24(5), 1135-1150, 2020

Modelling of Remazol Black-B Adsorption on Chemically Modified Waste Orange Peel: pH Shifting Effect of Acidic Treatment

Ceren KARAMAN*[1], Zümriye AKSU[2]

Abstract

The adsorption of Remazol Black-B (RBB) onto two different types of agricultural waste derived-adsorbents; dried-orange peel (DOP) and chemically modified orange peel (CMOP), was performed. The adsorption rate, capacity, and the dye removal efficiency were investigated in terms of initial pH ranged between 2.0 to 10.0 of the dispersion and the operating temperature of 25 °C, 35 °C, 45 °C . The Langmuir and Freundlich adsorption models were applied to the experimental data to model the adsorption equilibrium, and evaluated by regression analysis. The results indicated that the Langmuir model was more suitable to describe the adsorption equilibrium of RBB over CMOP. According to Langmuir model, while the highest RBB uptake capacity of DOP was determined as 62.4 mg.g^{-1} at pH 2.0 and 25°C, this value was figured out for CMOP as 84.4 mg.g^{-1} at pH 8.0 and 45°C. Furthermore, the adsorption kinetics followed both the pseudo-second order and the saturation type kinetic models for each adsorbent-dye system. The thermodynamic parameters of adsorption including the Gibbs free energy change (ΔG^o), the enthalpy change (ΔH^o), and the entropy change (ΔS^o) were obtained by using thermodynamic equations. These parameters were calculated as -4.24 kJ.mol^{-1}, 43.77 kJ.mol^{-1}, 0.16 kJ mol^{-1}.K^{-1} for CMOP respectively whereas for DOP -3.58 kJ.mol^{-1},-19.79 kJ.mol^{-1}, -0.05 kJ mol^{-1}.K^{-1} .

Keywords: Adsorption, Orange Peel, Remazol Black-B, Acidic Treatment, Chemical Modification, pH shifting, Agricultural Waste

1. INTRODUCTION

Since industrial wastewaters contain large amount and different types of pollutants such as dyes, surfactants, heavy metals and salts, they are one of the greatest threats to the environment. Among these pollutants, dyes, and pigments used in many industries (i.e., textile, pharmaceutical, paper, plastic, petrochemical etc.) lead to severe harmful effects both to the ecosystem and to human health. Due to their synthetic origins and complex molecular structures, it is difficult to biodegrade dye effluents. These effluents not only significantly reduce sunlight penetration but also decrease the solubility of oxygen in the water. As a result, the photosynthetic activity of living

* Corresponding Author: cerenkaraman@akdeniz.edu.tr
[1] Akdeniz University, ORCID: http://orcid.org/0000-0001-9148-7253
[2] Hacettepe University, E-Mail: zaksu@hacettepe.edu.tr ORCID: http://orcid.org/0000-0002-2812-5345

organisms in the aquatic system is inhibited [1]. Therefore, removal of the dyes from wastewater before discharge into the environment is essential for the protection of the environment and human health. In order to contribute to the total solution of this problem, in addition to conventional technologies (like coagulation, flocculation, precipitation, ozonation, etc.), several treatment technologies have gained prominences, such as membrane processes, electrochemical techniques, photocatalytic oxidation/degradation, adsorption and combined methods [2]. Amongst them, adsorption processes generally have high removal efficiency and can be scaled-up [3]. Furthermore, adsorption attracts more attention because it allows the adsorbent regeneration, which is an important economic advantage [4].

In the last decades, plenty of research groups have been tried to develop alternative adsorbents, which are economic, environmentally friendly and reusable, to desalination the wastewater. To call an adsorbent as "alternative adsorbent", it should be a waste or by-product of an industrial process. Besides, it should be plenty in nature or to be processed easily [5]. In light of this definition, agricultural wastes/by-products can be considered as the most important candidate of an alternative low-cost, non-toxic adsorbent for the removal of different kinds of contaminants such as dyes, heavy metals, and organics. They are lignocellulosic materials which mainly consist of cellulose, lignin, and hemicellulose. There are many studies which investigate the performance of agricultural waste/by-products to remove dyes or heavy metal ions from wastewater, peach stone [6], cherry stones [7], coconut shell [8-10], walnut shell, coffee bean husk, corn cob, rice husk, pecan shell and sugar cane bagasse [11,12].

In this study, the potential use of waste orange peel, one of the valued lignocellulosic agricultural wastes discharged from juice industry, and its derivative type, chemically modified orange peel, was investigated as an adsorbent for anionic reactive dye, RBB. Owing not only to its high content of different functional groups, such as carboxyl and hydroxyl groups but also to its lignocellulosic content such as of lignin, cellulose, hemicellulose, pectin and others, waste orange peels can be used as a satisfactory adsorbent [13-15]. Although utilization of waste orange peels as adsorbents for removal of effluents in industrial wastewaters is one of the studies explored in literature, as far as the authors' knowledge, there seems to be no study which uses the chemically modified orange peel to remove textile dyes. This paper presents the outcomes about the application of DOP and CMOP as adsorbents for the removal of RBB from aqueous solution.

In this study, the effects of the temperature and the initial pH of the adsorption system on the RBB removal performance of orange peel derived adsorbents (DOP and CMOP) were investigated. Although some studies using the waste orange peel as an adsorbent have been published, especially the equilibrium, kinetic and thermodynamic modelling of RBB adsorption onto the chemically modified orange peel has not been studied comprehensively yet. Since the modelling of the adsorption process assists in optimizing the process' conditions, the Langmuir and Freundlich adsorption models were used to express adsorption of RBB in aqueous media and the effect of temperature on the model constants was evaluated. Moreover, because the thermodynamic parameters are also crucial in the design of the treatment processes, these fundamental data were calculated for further applications.

2. MATERIALS AND METHODS

2.1. Reagents and Preparation of Test Solutions

RBB supplied by Sigma-Aldrich was used without additional treatment (Figure A1.). The examples with the initial dye concentration range between 25 and 750 $mg.L^{-1}$ were prepared by diluting 1.0 $g.L^{-1}$ of RBB dye stock solution. The initial pH of each solution was set to the desired value by using 0.1 N HCl and 0.1 N NaOH solutions before introducing the adsorbent.

2.2. Adsorbent Preparation

The waste orange peels were obtained from the BELSO fruit juice production facility Ankara, Turkey, and they were washed with a large volume of tap water, followed by deionized (DI) water. Subsequently, they dried in a vacuum oven at 70 °C for 24 h. After ball milling, the adsorbents with 500-707 µm particle size range were stored in airtight containers ready for further use as the adsorbent named dried orange peel (DOP). During the acidic treatment of the DOP, an isothermal reactor unit consisting of a pyrex glass and a condenser was used. 1.0 g DOP was added to 250 mL of 1.0 M H_2SO_4 solution. The acidic treatment reaction was conducted for 6 hours at 25 °C. The hydrolysate fluid was then removed from the solid by centrifugation. The solid was washed DI water to reach a neutral pH and then dried at 75 °C in a vacuum oven for overnight. The acidic treated orange peels were stored in airtight containers ready to use as the adsorbent, named chemically modified orange peel (CMOP).

2.3. Characterization of The Adsorbents

The surface morphologies of the adsorbents were characterized by Hitachi S-4900 FE-SEM operating at 5.0 kV. The N_2 adsorption/desorption measurements (at 77 K) were performed by Quantachrome Nova 2200 automated surface area analyzer (Quantachrome Corporation, USA). The isotherm data supplied from N_2 adsorption/desorption experiments were applied to the Brunauer–Emmett–Teller (BET) theory for specific surface area. Pore size distributions (PSD) were measured based on the Barrett-Joyner-Halenda (BJH) method.

2.4. Evaluation of The Uptake Performance

Adsorption experiments were conducted by the batch technique in an Erlenmeyer (Pyrex glass) containing 100 mL of RBB solution. The experimental samples were placed in an incubator at a shaking rate of 100 rpm and set to the temperature of 25 °C, 35 °C, 45 °C, respectively. All of the adsorption studies were carried out for 24 h to reach the equilibrium conditions. For the adsorption studies, 0.1 g of DOP or CMOP was added to 100 mL of the dye solution, and this moment was defined as t_0. Subsequently, at pre-determined time intervals, periodically 5 mL of samples were taken from the system and centrifuged at 4000 rpm for 10 min. Then, the amount of dye uptake, percentage of dye removal, and adsorption rate values of the adsorbent were calculated with the help of Equations (1-3).

$$q = \frac{(C_0 - C)}{X} \quad (1)$$

$$\%\ \text{removal efficiency} = \frac{(C_0 - C)}{C_0} \times 100 \quad (2)$$

$$r_{ad} = \frac{\Delta q}{\Delta t} \quad (3)$$

Where q ($mg.g^{-1}$) is the adsorption capacity; C_o ($mg.L^{-1}$) is the initial RBB concentration; C ($mg.L^{-1}$) is the residual dye concentration at any time of the adsorption procedure; X is the adsorbent concentration ($g.L^{-1}$); r_{ad} the adsorption rate of the adsorbent ($mg.g^{-1}\ min^{-1}$); t is the time (min).

The concentrations of RBB remaining in the aqueous phase were analyzed by UV-Vis spectrophotometer at the maximum adsorption peak (λ_{opt}) of 598.0 nm obtained experimentally for RBB. In order to determine the remaining RBB concentration in the aqueous phase, the calibration curve obtained experimentally for different RBB concentrations was used. All the experiments were repeated twice to verify the repeatability and accuracy, and the average of them were used for further calculations.

2.4.1. Effects of initial pH

Since the initial pH of the adsorption media affects the surface charge of the adsorbent, the ionization of the dye molecules or dissociation of the dye ions in the bulk solution, and also the interactions between the functional groups and unsaturated bonds, it is crucial to optimize the initial pH [1,16]. The effect of pH on the adsorption capacity of the adsorbent was investigated at the pH values of 2.0, 3.0, 4.0, 5.0, 6.0, 8.0, 10.0 at 25 °C, and at initial RBB concentration of 25 $mg.L^{-1}$.

2.4.2. Effects of initial RBB concentration and operation temperature

The effects of initial RBB concentration and operation temperature on the adsorption were investigated at initial dye concentrations of 25 $mg.L^{-1}$, 50 $mg.L^{-1}$, 100 $mg.L^{-1}$, 250 $mg.L^{-1}$, 500 $mg.L^{-1}$, and 750 $mg.L^{-1}$ and at operating temperatures of 25 °C, 35 °C, 45 °C. Each experiment was conducted at the optimum pH values for each adsorbent determined according to Section 2.4.1.

2.5. Modelling of The Adsorption

2.5.1. Modelling of adsorption kinetics: Application of simplified kinetic models

Since the adsorption is a time-dependent equilibrium process, it is important to well define the adsorption rate to control and to evaluate the process. To express the adsorption rate, simplified kinetic models including pseudo-first order, pseudo-second order and saturation type kinetic models were applied to the experimental data. The linearized equations of these models were depicted in Table A1. According to these linearized equations, to validate the applicability of pseudo-first order kinetics, the plot of t/q vs. t should give a linear relationship, with the help of this graph q_{eq} and $k_{2.ad}$ can be calculated from the slope and the intercept of the plot (Table A1).

2.5.2. Modelling of adsorption equilibrium: Application of adsorption equilibrium models

At equilibrium conditions of the adsorption process, the amount of effluent at the solid-liquid interface (q_{eq}) increases non-linearly with the concentration. To determine the maximum adsorption capacity of the adsorbent and to identify the type of adsorption equilibrium, the Langmuir and the Freundlich adsorption isotherms (two-parameter models) were applied to experimental data at different temperatures for each adsorbent-dye system. The non-linear equations of these models were presented in Table A2.

The Langmuir equation is valid for monolayer adsorption and has some assumptions as following: *(i)* the adsorbent surface has a finite number active sites and all of these sites have the same adsorption energy (a homogenous surface); *(ii)* the adsorption process is reversible; *(iii)* there is no interaction between the adsorbed species; *(iv)* if an active site on the adsorbent absorbs an adsorbate, there is no way to occur another adsorption on that site [17]. According to this model, as the saturation of the adsorption is reached, no further binding sites are available on the adsorbent surface and the maximum adsorption capacity (Q^0) corresponding to complete monolayer coverage on the sorbent surface is obtained. The Langmuir model constants are significantly dependent on the adsorbent type and temperature. The linearized Langmuir model can be expressed in the form of Equation (4),

$$\frac{C_{eq}}{q_{eq}} = \frac{C_{eq}}{Q^0} + \frac{1}{Q^0 b} \quad (4)$$

where Q^0 ($mg.g^{-1}$), represents the maximum saturated monolayer adsorption capacity (maximum amount of adsorbate adsorbed per gram of adsorbent) under the given conditions. According to Equation (4), a plot of $1/q_{eq}$ vs. $1/C_{eq}$ should give a straight line with a slope of Q^0, and an intercept of b. The Langmuir model constant b is related to the free energy of adsorbent and shows the affinity of the adsorbent for the binding of effluent.

Unlike the Langmuir model, the Freundlich empirical equation is based on the adsorption onto a heterogeneous adsorbent surface affected by temperature. This model suggests neither linearity at low effluent concentration nor a fixed adsorption capacity as any saturation is reached. According to this model, the multilayer adsorption on the heterogeneous adsorbent surface is occurred [18]. As a result, an exponential shaped theoretical equilibrium curve is obtained. The linearized form of the Freundlich model equation is given as in Equation (5),

$$\ln q_{eq} = \ln K_F + \frac{1}{n} \ln C_{eq} \quad (5)$$

A linear plot of $log\ q_{eq}$ vs. $log\ C_{eq}$ was plotted to determine the n (adsorption intensity) and K_F (adsorption capacity) model constants with the

help of the slope and the intercept of the graph, respectively. The higher *n* value means the stronger adsorption intensity, and generally, n>1 indicates that adsorbate is favorably adsorbed on the adsorbent [19]. K_F, is one of the Freundlich model constants related to the adsorption capacity of the adsorbent.

2.5.3. Modelling of adsorption thermodynamics

In the adsorption process, it is important to establish the adsorption mechanism such as chemical or physical adsorption. While during physical adsorption, the relatively weak interaction is taken into account, in chemisorption stronger chemical interactions take place [17]. To distinguish the physical and chemical adsorption, it is essential to determine the thermodynamic parameters, including the Gibbs free energy change (ΔG^o; kj mol^{-1}), the enthalpy change (ΔH^o; kj mol^{-1}), and the entropy change (ΔS^o; kj mol^{-1}K^{-1}) in the system.

The Gibbs free energy of the system can be obtained using the following relationship;

$$\Delta G^o = -RT \ln K_c^o \quad (6)$$

where K_c^o is the thermodynamic equilibrium constant, *R is* is the universal gas constant (8.314 J.mol^{-1}K^{-1}) and *T* is the temperature (*K*). Since the adsorption process is a heterogeneous equilibrium process, it can be summarized by the reversible process between the effluent in solution and the effluent-adsorbent. The apparent equilibrium constant (K_c') of this system can be defined as;

$$K_c' = \frac{C_{ad,eq}}{C_{eq}} \quad (7)$$

where $C_{ad,eq}$ is the concentration of the effluent on the adsorbent at the equilibrium. In this case, instead of the concentration values, the activity of the species can be used to obtain standard thermodynamic equilibrium constant (K_c^o) of the adsorption system. This value can be obtained by calculating K_c' at different initial effluent concentrations and extrapolating data to zero. It will be also equal to the *1/intercept* of C_{eq}/q_{eq} vs. C_{eq} graph ($=bQ^o$) at 25 ºC, which indicates the linearized form of the Langmuir adsorption model equation.

According to the law of thermodynamics the relationship of ΔG^o to ΔH^o and ΔS^o can be expressed as:

$$\Delta G^0 = \Delta H^o - T\,\Delta S^0 \quad (8)$$

Moreover, the relationship between the K_c^o and *T* is obtained by Equation (6) into Equation (8) and called as the van't Hoff equation:

$$\ln K_c^o = \frac{\Delta S^o}{R} + \frac{\Delta H^o}{R\,T} \quad (9)$$

The enthalpy change and the entropy change of the system can be computed according to the linearized van't Hoff plot of ln K_c^o vs. *1/T.*

3. RESULTS AND DISCUSSIONS

3.1. Characterization of The Adsorbents

Figure 1a-b show that DOP exhibited irregular shape bulk-like carbon monoliths with a smooth surface where no cavities or holes detected. On the other hand, CMOP presented a well-developed porous and interconnected network with abundant micro and mesoporous structure (Figure 1c, and d) which my be attributed to etching effect of acidic treatment .

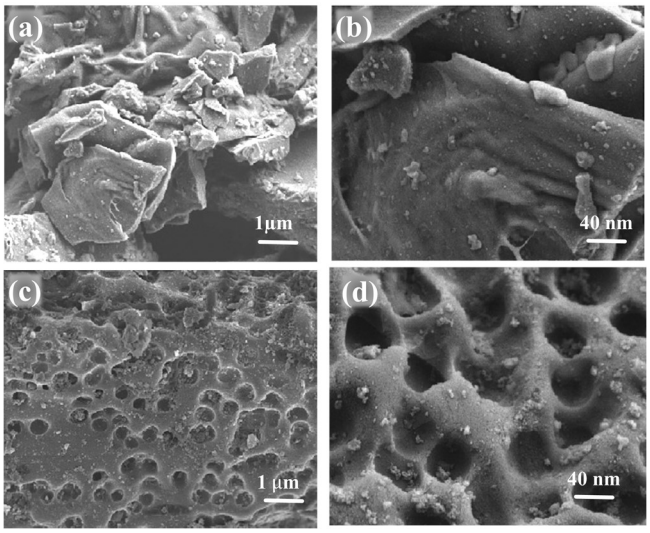

Figure 1 FE-SEM images of (a,b) DOP, and (c,d) CMOP at the same magnifications

The porous structure of the DOP, and CMOP was analyzed by the N_2 adsorption/desorption

isotherms. As shown in Figure 2a, DOP presented essentially a Type-I isotherm which confirms the presence of dominant microporous structure [20]. This was also confirmed by the pore size distribution curve (Figure 2b) calculated by the BJH method. On the other hand, CMOP exhibited type-IV isotherm with an H4 type hysteresis loop located between 0.40 and 0.99 of P/P^0, according to the presence of mesoporous carbon structures [21]. Furthermore, a sharp increase of N_2 uptake at a relative pressure of <0.1 proves the existence of micropores. Chemical modification improved S_{BET} and porosity structure of DOP, as presented in Table 1. While S_{BET} value of DOP is merely 102.0 $m^2.g^{-1}$, consisting of very low pore volume, after chemical treatment, the surface area and pore volume was enhanced to 651.0 $m^2.g^{-1}$ and 0.625 $cm^3.g^{-1}$ (Table 1), respectively. These results proves that acidic treatment was an effective method for synthesis of well-ordered porous carbon structure with high porosity.

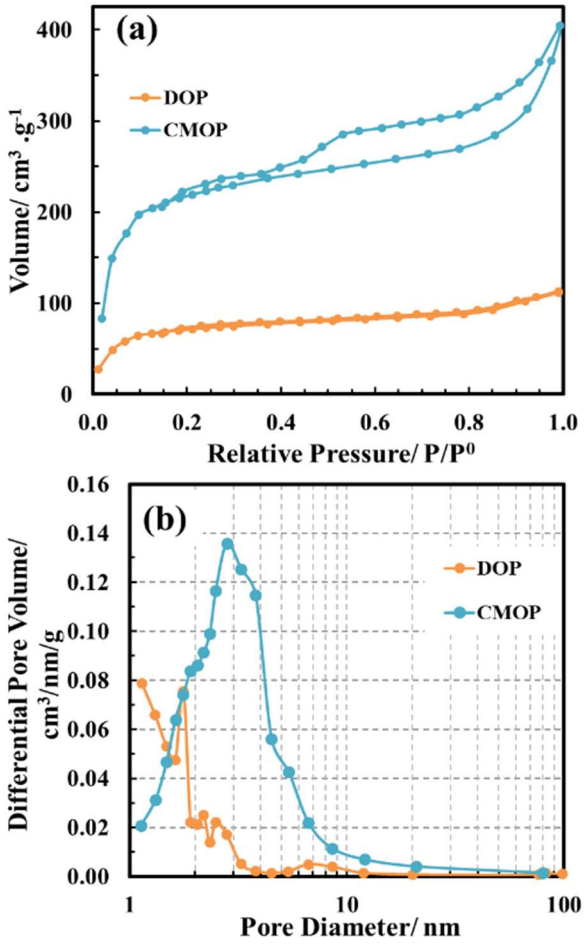

Figure 2 (a) N_2 adsorption/desorption isotherms, and (b) the BJH pore size distributions of DOP and CMOP

Table 1
Physicochemical parameters obtained from N_2 adsorption/desorption isotherms of DOP and CMOP samples

Sample ID	S_{BET} $m^2.g^{-1}$	V_{micro} cm^3/g	V_{meso} cm^3/g	V_{total} cm^3/g	% V_{micro}	% V_{meso}
DOP	102.0	0.095	0.046	0.141	67.38	32.62
CMOP	651.0	0.258	0.394	0.652	39.55	60.45

3.2. Evaluation of the Uptake Performance

3.2.1. Effects of initial pH

As shown in Figure 3, the pH dependence of the adsorption capacity of both DOP and CMOP were investigated at 100 $mg.L^{-1}$ initial dye concentration between the pH range out from 2.0 to 10.0. It can be seen that the dye removal of each adsorbent was strongly depended on the initial pH. While the highest uptake of DOP was obtained at pH 2.0 as 19.4 $mg.g^{-1}$, this value for CMOP was shifted to pH 8.0, almost neutral, as 30.4 $mg.g^{-1}$ for the uptake of RBB (Figure 3). However, it should be taken into consideration that natural wastewaters generally have pH values higher than acidic values (pH >2). the pH values close to the natural pH value are more relevant results due to easy and direct application to the system of interest. The results verified that the DOP mainly consists of negatively charged surface functional groups such as carboxyl groups, nitrogen-containing functional groups, and some weaker acidic groups. Just as the pH of the system decreases, the adsorbent surface charges more positively. Thus, the RBB adsorption capacity of the DOP turns out more favorable owing to the electrostatic attractions between RBB anions and positively charged adsorbent surface. DOP charged more positively for pH values lower than 3.5-4.0 because of the ionization of the surface functional groups and charged more negatively at higher pH values. At acidic medium, most of the potential active sites of the adsorbent are protonated so the maximum adsorption capacity of DOP was obtained at pH 2.0 [5]. This result is also supported by the other researchers that the surface functional groups of the adsorbent may become protonated under relatively acidic media [22-25]. According to some researchers, nitrogen containing functional

groups show significant potential for the removal of reactive dyes from aqueous solution due to the electrostatic interactions between amine groups of the adsorbate and sulfonate groups of the RBB [16, 26].

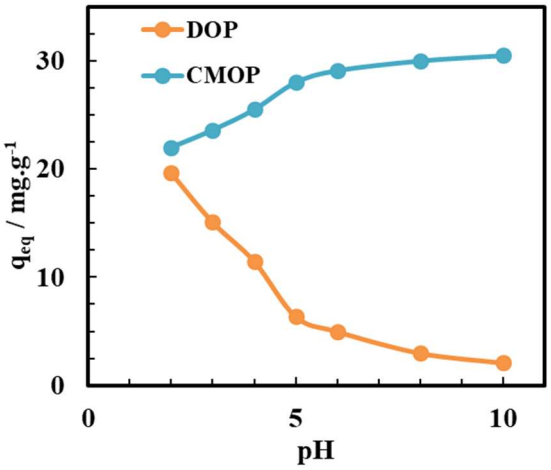

Figure 3 Effect of the initial pH of the solution on the equilibrium uptake of RBB (C_o: 100 mg l^{-1}, T: 25 ˚C, agitation rate: 100 rpm)

As the pH is shifted to the alkaline region, while the number of positive surface charges decreases, the increment is observed in the amount of negatively charged surface sites. As a result of the electrostatic repulsion, this situation does not favor the adsorption of RBB anions on the adsorbent dominated by negative sites. The competition between the OH^- ions increased by the higher pH value and the RBB anions for the adsorption onto the active sites leads to decrease of the adsorption capacity of the adsorbent. It is suggested that as a result of acidic treatment of DOP, the surface charge has been changed anionic to cationic. The chemical modification of DOP by acidic treatment leads to a change of surface charge negative to positive, which therefore indicates that CMOP added favorable electrostatic contribution to RBB around the natural pH range. These findings also support the results related to the pH dependence of RBB adsorption capacity of the adsorbent represented in Figure 3. In the light of these results it can be suggested that the adsorption process of the RBB onto each adsorbent probably consist of two steps; electrostatic interaction and then ion-exchange or complexation between adsorbent and adsorbate.

3.2.2. Effect of initial RBB concentration and operation temperature

For different initial RBB concentration and operation temperature, each adsorbent showed different behavior (Figure 4). At all temperatures, adsorption on each adsorbent was enhanced significantly by increasing the initial RBB concentration tending to saturation at higher dye concentrations. Increasing the dye concentration provides a considerable driving force to eliminate the effect of mass transfer resistances of the dye between solid-liquid interfaces. Moreover, the number of interactions between the adsorbent and the adsorbate relatively increase by the initial dye concentration, which enhances the RBB removal capacity of the adsorbent. However, the removal RBB efficiency of each adsorbent does not increase with the initial dye concentration. At all temperatures studied, RBB removal % was higher at lower dye concentrations for each adsorbent due to the availability of unoccupied active sites on the surface of the adsorbents. Increasing the dye concentration diminished the dye removal efficiency, due to almost filled active sites of the adsorbents.

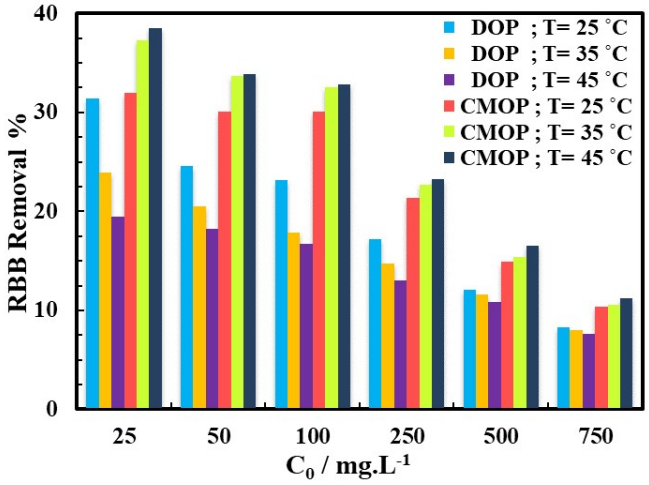

Figure 4 Effects of temperature and the initial dye concentration (C_0 ; $mg.L^{-1}$) on RBB removal efficiency of DOP; at pH=2.0 and CMOP at pH=8.0

Temperature is another parameter which plays a crucial role in both the adsorption rate and the equilibrium dye uptake of adsorbents. The results obtained for DOP revealed that the adsorption behavior of DOP indicated an exothermic character and q_{eq} values diminished with the

increasing temperature. As adsorption generally is an exothermic process, this is expected due to the weakened physical bounding with increasing temperature. At 100 mg.L^{-1} initial dye concentration with increasing temperature from 25 ℃ to 45 ℃, while the equilibrium uptake capacity of DOP decreased from 23.3 mg.g^{-1} to 16.7 mg.g^{-1}, that of CMOP increased from 30.4 mg.g^{-1} to 36.6 mg.g^{-1}. The decrease in adsorption of DOP at higher temperature may be referred to the deactivation of the active sites on the adsorbent surface (Table 2). As listed in Table 2, the data obtained from adsorption of RBB on CMOP demonstrated that the adsorption performance of the adsorbent was favored by the increase of the temperature, so the results showed that the adsorption of RBB by CMOP was endothermic. The change of the adsorption characteristic from exothermic to endothermic behavior revealed that the chemical modification by acidic treatment of the DOP led to change the surface charge and the structure. The enhancement of the adsorption capacity could be attributed to an increase in the number of active sites on the surface available for the adsorption, increase in the porosity and the total pore volume of the adsorbent (Figure 2). It may also be attributed to the decrease in the mass transfer resistance with decreasing the thickness of the boundary layer surrounding the adsorbent . Furthermore, the kinetic energy of the molecules, namely the mobility of the RBB molecules increases with the increasing of the temperature. Consequently, the dye molecules can easily transport from the bulk solution to the adsorbent-solution interface, so this may easily enhance the rate of intra-particular diffusion of adsorbate [19]. It can be concluded that the adsorption of RBB on the CMOP may involve not only the physical adsorption but also the chemical adsorption.

Table 2
Effect of temperature and initial dye concentration on adsorption rate (r_{ad}), equilibrium uptake of RBB (q_{eq}), and RBB removal % for DOP and CMOP (X: 1.0 g.L^{-1}, and agitation rate: 100 rpm)

		DOP at *pH= 2.0*			**CMOP at *pH= 8.0***		
T (℃)	**C_o (mg.L^{-1})**	**r_{ad} (mg.g^{-1}min^{-1})**	**q_{eq} (mg.g^{-1})**	**RBB Removal %**	**r_{ad} (mg.g^{-1}min^{-1})**	**q_{eq} (mg.g^{-1})**	**RBB Removal %**
25	25	0.14	7.4	31.4	0.25	7.9	32.0
	50	0.24	12.4	24.6	0.46	14.6	30.1
	100	0.51	23.3	23.2	0.73	30.4	30.1
	250	0.87	43.3	17.2	1.13	54.1	21.4
	500	1.23	61.1	12.1	1.37	75.2	14.9
	750	1.45	62.4	8.3	1.48	78.5	10.4
35	25	0.12	6.1	23.9	0.26	8.3	37.3
	50	0.21	10.2	20.5	0.49	16.4	33.7
	100	0.43	18.1	17.9	0.79	33.1	32.5
	250	0.75	37.3	14.7	1.18	56.1	22.7
	500	1.12	59.2	11.6	1.44	771	15.4
	750	1.29	60.5	8.0	1.55	79.6	10.6
45	25	0.11	5.2	19.5	0.29	8.1	38.5
	50	0.19	9.3	18.2	0.52	17.1	33.9
	100	0.42	16.7	16.7	0.84	36.6	32.8
	250	0.72	33.1	13.0	1.24	58.3	23.3
	500	1.09	54.8	10.8	1.49	82.2	16.5
	750	1.27	57.3	7.6	1.59	84.4	11.2

Figure 5 demonstrated the adsorption kinetics of RBB, at all temperatures by plotting the uptake capacity (q) vs. time (t) for 25 mg.L^{-1} and 750 mg.L^{-1} initial RBB concentrations for the first 7 h of the adsorption.

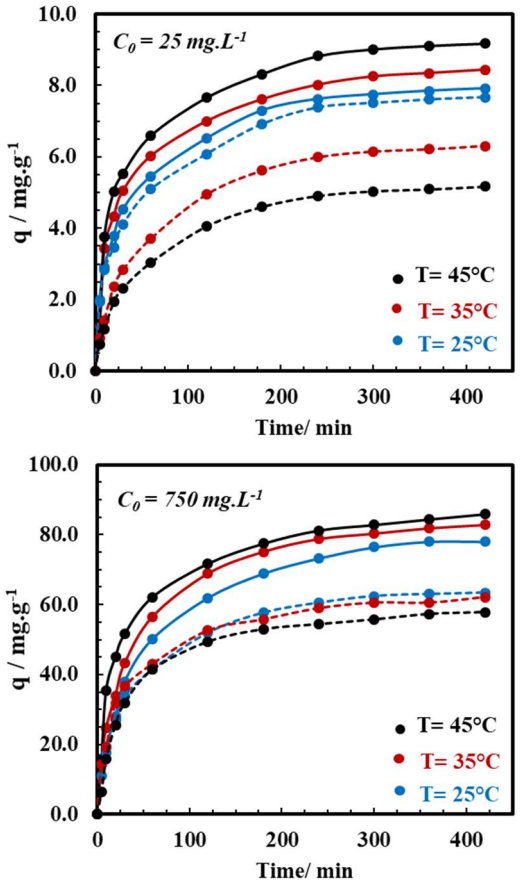

Figure 5 The adsorption equilibrium curves of RBB at different initial dye concentrations (C_0) and at different temperatures for DOP (dashed lines) and CMOP (Straight lines) at pH= 2.0 and pH=8.0, respectively

Figure 5 shows a contact time from 2 to 4 h depending on the temperature and the adsorbent was sufficient to reach equilibrium. The adsorption level did not change subsequently up to 24 h. At the beginning of the adsorption process, the RBB uptake capacity of the adsorbents increased with the contact time linearly, then non-linearly got to a slower rate and at the end, the adsorbent achieved the saturation called the equilibrium time and equilibrium uptake capacity (q_{eq}). Moreover, it was noticed that at all temperatures for all initial RBB concentrations, the majority of RBB adsorption onto each adsorbent (~ 60 - 70 %) took place within the first two hours of the whole process (Table 2). Both DOP and CMOP have an affinity for RBB and the uptake of RBB occurs mainly by surface binding. The number of available active sites of the surface is the limiting factor for the adsorption [19]. CMOP showed higher uptake of RBB than DOP at all temperatures due to its surface characteristics, especially specific surface area, number of active sites, surface charge, the total pore volume and pore size distribution (Table 1).

3.3. Modelling of The Adsorption

3.3.1. Modelling of adsorption kinetics: Application of simplified kinetic models

The adsorption rate constants ($k_{1.ad}$ and $k_{2.ad}$) and theoretical equilibrium uptake capacities ($q_{eq.cal}$) of each adsorbent were obtained for each adsorbent-dye system (Table 3).

Table 3
Comparison of the experimental and calculated q_{eq} values for the pseudo-first order and pseudo-second order adsorption kinetics at different temperatures of RBB concentration of 100 mg.L^{-1}

	T (°C)	C_o (mg.L^{-1})	$q_{eq.exp}$ (mg.g^{-1})	Pseudo-first order kinetic model			Pseudo-second order kinetic model		
				$q_{eq.cal}$ (mg.g^{-1})	$k_{1.ad}$ (min^{-1})	R^2	$q_{eq.cal}$ (mg.g^{-1})	$k_{2.ad}$ x10^3 (g.mg^{-1}min^{-1})	R^2
DOP at pH=2.0	25	100.5	23.31	17.91	0.0143	0.962	23.81	2.03	0.998
	35	100.9	18.09	13.31	0.0127	0.939	17.92	1.82	0.993
	45	99.0	16.69	14.04	0.0124	0.989	16.89	1.75	0.999
CMOP at pH=8.0	25	101.0	30.4	25.9	0.0189	0.923	31.5	1.08	0.999
	35	101.9	33.1	25.4	0.0233	0.946	32.4	1.11	0.999
	45	105.4	36.6	33.5	0.0240	0.943	37.9	1.29	0.999

As indicated in Table 3, for both of the adsorbents, the correlation coefficients (R^2) for pseudo-second-order kinetic were calculated much higher than those calculated for the pseudo-first-order kinetic. It was concluded that the pseudo-second order kinetic model fits better the experimental data obtained for RBB adsorption onto both adsorbents for the entire adsorption period suggesting chemisorption mechanism. Besides the pseudo-first order and pseudo-second order kinetic models, the saturation type kinetic model was also applied to experimental data to describe the batch adsorption kinetics over the entire concentration range of RBB and all temperatures studied as presented in Table 4.. Table 4 shows that this kinetic model was also well fitted with the experimental data to express the adsorption kinetics of RBB on DOP and CMOP (plots not shown). It was observed that the adsorption rate constants were affected by the temperature. The change of the rate constants with the temperature indicated that adsorption reaction was one of the rate controlling steps of the whole process. All of these findings suggested that the adsorption of RBB at 25- 45 ˚C could be best described by the pseudo-second order kinetics and saturation type kinetic model, with high correlation coefficients.

Table 4
The saturation type kinetic rate constants obtained at different temperatures for different adsorbents

	T (˚C)	k_{ad} x 10^2 ($L.g^{-1}min^{-1}$)	$k_{o,ad}$ x 10^2 ($L.mg^{-1}$)	R^2
DOP at pH=2.0	25	6.22	0.30	0.998
	35	4.91	0.25	0.999
	45	4.46	0.21	0,998
CMOP at pH=8.0	25	1.24	0.72	1.000
	35	1.37	0.80	1.000
	45	1.42	0.82	0.999

3.3.2. Modelling of the adsorption Equilibrium: Application of adsorption equilibrium models

According to the linearized Langmuir model equation (Equation 4), the theoretical maximum adsorption capacity (Q^0) of RBB on DOP and CMOP were obtained as 63.30 $mg.g^{-1}$ at 25 ˚C, and 89.30 $mg.g^{-1}$ at 45 ˚C, respectively. At all temperatures, Q^0 values were calculated higher for the CMOP-RBB system in comparison with the DOP-RBB system. The higher b value indicates the higher affinity of the adsorbents for the adsorbate [18]. Similarly, the b values for CMOP were much higher than that of DOP at all temperatures investigated (Table 5).

Table 5 The Langmuir and the Freundlich adsorption isotherm parameters for RBB adsorption on DOP and CMOP at various temperatures

		The Langmuir Model Constants				**The Freundlich Model Constants**			
	T (˚C)	Q^o ($mg.g^{-1}$)	b	R^2	ε (%)	K_F [$(mg.g^{-1})(mg.L^{-1})^n$]	n	R^2	ε (%)
DOP at pH=2.0	25	63.30	0.0073	0.9987	2.2	1.67	1.5	0.9780	8.2
	35	61.70	0.0050	0.9989	2.2	1.49	0.9	0.9998	6.7
	45	57.80	0.0048	0.99991	1.9	1.41	0.7	0.9886	8.5
CMOP at pH=8.0	25	78.10	0.0713	0.99986	3.4	1.69	2.2	0.9947	16.5
	35	82.60	0.1122	0.99987	2.3	1.72	2.8	0.9958	15.5
	45	89.30	0.1894	0.99990	2.2	1.75	3.7	0.9977	13.2

K_F values calculated for each adsorbent showed that RBB adsorption capacity of CMOP relatively higher than DOP (Table 5). A higher value of K_F indicates that a higher adsorption capacity. Although the K_F increased with an increase in the temperaturefor CMOP, it decreased for DOP. It was also observed that while all n values obtained for CMOP were greater than unity, these values for DOP was greater only at 25 ˚C than unity (Table 5). These results indicated that RBB was more favorably adsorbed by CMOP at all temperatures studied. The non-linearized adsorption isotherm models for the fitting of RBB adsorption on DOP and CMOP were plotted as graphs of q_{eq} vs. C_{eq} at different temperatures (Figure 6). The overlapping of the experimental and the non-linearized model curves was an evidence that the Langmuir adsorption model closely agreed with the equilibrium data for each adsorbent-dye system.

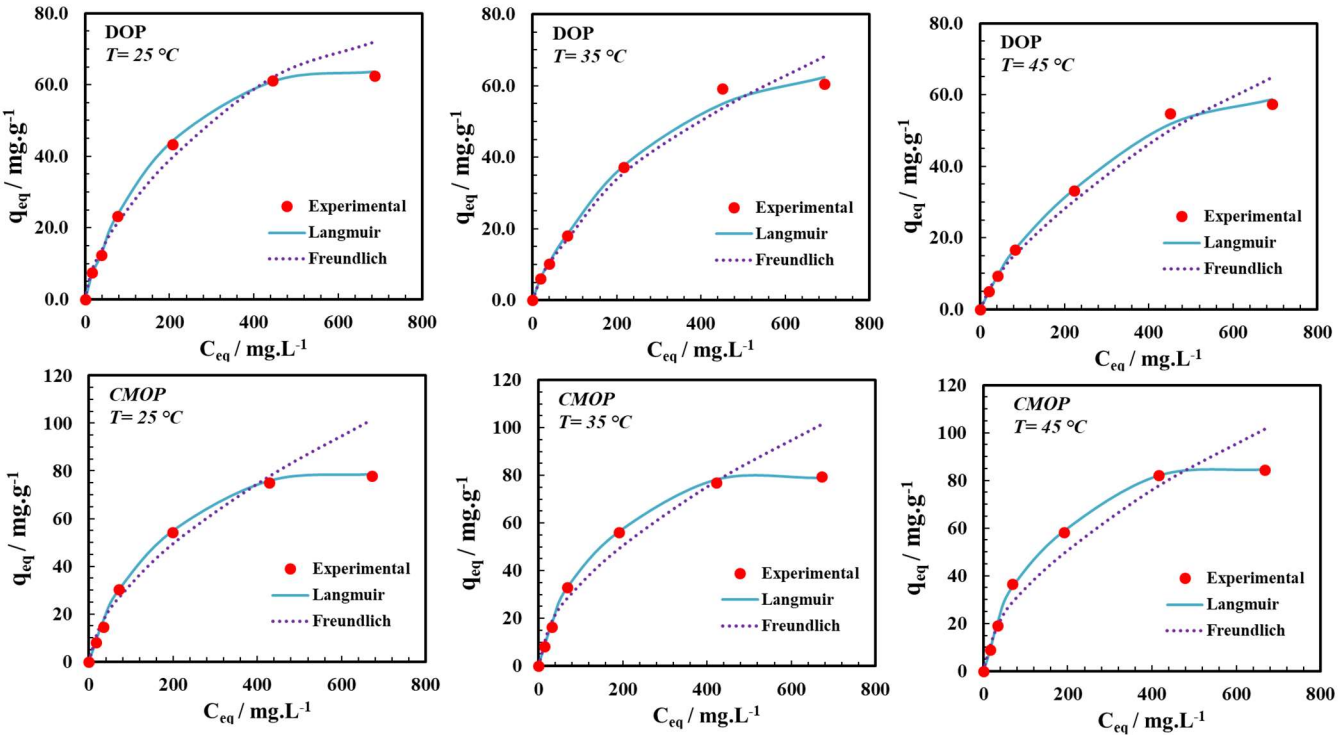

Figure 6 The experimental and estimated non-linearized adsorption isotherms of RBB on DOP, at pH= 2.0 and CMOP, at pH=8.0 at different temperature

In Table 5, the adsorption model parameters calculated by related model equations (Equation (4) and (5)), the linear regression coefficients (R^2) and average percentage error values (ε) were also presented. It was obvious that the Langmuir adsorption isotherm model well fitted the experimental data with much higher R^2 values, than that of the Freundlich model (Table 5 and Figure 6). On the other hand, the linear regression coefficients (>0.97) indicated that the Freundlich model was comparable to the Langmuir model. Another criterion for determination of the most applicable isotherm model is the magnitude of average percentage error values (ε) which show the deviation from the experimental q_{eq} values. On the basis of the ε values, it was proven the adsorption equilibrium data of RBB fitted very well to the Langmuir model in the initial dye concentration and temperature ranges investigated for each adsorbent. With an average percentage error values more than 6.7%, it was concluded that the Freundlich model exhibited a relatively poor fit to the adsorption data of RBB onto each adsorbent. The applicability of the Langmuir model indicated that the adsorption process of RBB was monolayer and had constant adsorption energy.

Table 5 also demonstrated that both of the model constants of CMOP increased with the temperature rise, which means that the RBB adsorption phenomenon on CMOP is governed by

an endothermic process, whereas RBB adsorption onto DOP showed exothermic character. The typical physical adsorption shows exothermic character. The weak electrostatic forces between the opposite charged sites on the adsorbent and effluent species in the solution are responsible for the adsorption behavior [17].

3.3.3 Modelling of adsorption thermodynamics

All of the thermodynamic parameters of each adsorbent-dye system were obtained by using the thermodynamic relationships and represented in Table 6. Generally, increasing of the adsorption capacity with the increasing temperature reflects the exothermic character of the adsorption process. This situation leads to negative standard enthalpy change of the process. Notably, an exothermic process is because the total energy released in bond occurred between effluent and the adsorbent is higher than the bond breaking, leading to release of extra energy in the form of heat [1, 2].

The standard thermodynamic equilibrium constant (K_c^o) of the adsorption system was obtained with the help of the linearized form of the Langmuir adsorption model equation (for detail see Section 2.5.3). The K_c^o values at 25 °C are calculated for DOP and CMOP as 4.2 and 5.5, respectively.

Table 6 shows that the signs of all thermodynamic parameters were in accordance with the experimental data of the adsorption isotherms. The negative value of enthalpy change reveals exothermic adsorption favorable at lower temperatures. It is demonstrated by a decrease in the maximum adsorption capacity of the adsorbent at higher temperatures. Meanwhile, the posi tive value of ΔH^0 for CMOP reflects that the endothermic nature of the adsorption process favorable at higher temperatures and possible relatively stronger bonding between the RBB and CMOP.

Table 6 Comparison of the thermodynamic parameters of RBB adsorption on DOP and CMOP

Adsorbent	ΔG^0 (kJ mol^{-1})	ΔH^0 (kJ mol^{-1})	ΔS^0 (kJ mol^{-1}K^{-1})
DOP (at pH=2.0)	-3.58	-19.79	-0.05
CMOP (at pH=8.0)	-4.24	43.77	0.16

Furthermore, both the magnitude and the sign of entropy change give the information about whether the adsorption process is occurred by an associative mechanism ($\Delta S^0<0$) or more randomly (a dissociative mechanism) ($\Delta S^0>0$). While the positive ΔS^0 value suggests that the high affinity of CMOP to RBB in solution and some structural changes or rearrangement in the dye-adsorption complex, the negative entropy change values confirm the decreased randomness and disorder at the solid-liquid interface during the adsorption of RBB onto CMOP. Furthermore, the positive entropy change indicated that the adsorption process was entropy-governed rather than enthalpy-governed. The negative ΔG^0 value implies that at all temperatures suggested that the adsorption process took place favorably and spontaneously.

4. CONCLUSIONS

This study has investigated the adsorption characteristics of the untreated waste orange peel-DOP and chemical pre-treated waste orange peel-CMOP adsorbents for the removal of RBB ions from the aqueous solutions. As a result of acidic treatment, the lignin, cellulose and hemicellulose structures in the DOP have been decomposed, the surface charge have changed negative to positive due to the acidic medium, and a highly porous structure has been obtained. The optimum pH value of the system has shifted from pH 2.0 to 8.0, almost natural, and the RBB uptake capacity of the adsorbent has been increased. The maximum adsorption capacity calculated according to the Langmuir model was determined as 62.4 mg/g at 25°C and pH 2.0 for DOP and this value was figured out for CMOP as 84.4 mg.g^{-1} at 45°C and pH 8.0 (35.2% higher). The Langmuir adsorption model provided more realistic description of RBB

onto both adsorbent-dye systems and could be used to predict the uptake of RBB with more accuracy than the Freundlich model for each system. The acidic treatment of DOP change the adsorption characteristic from exothermic to endothermic. The acidic treatment had shifted the structure of the DOP to shift the mechanism of the adsorption process from physical adsorption to the chemical adsorption with higher ΔH^0 value (>10 kJ $kmol^{-1}$).

The novel CMOP adsorbent, a widely available agricultural by-product, could be a promising candidate for practical applications as a low-cost and efficient agricultural waste adsorbent for anionic dye removal from the textile industry wastewater.

Funding

The authors received no financial support for the research, authorship, and/or publication of this paper.

The Declaration of Conflict of Interest/ Common Interest

No conflict of interest or common interest has been declared by the authors.

Authors' Contribution

CK: investigation, conceptualization, methodology, data curation, Writing- original draft preperation, Writing-reviewing and editing draft preparation, visualization ZA: Supervision, conceptualization, methodology, resources.

The Declaration of Ethics Committee Approval

The authors declare that this document does not require an ethics committee approval or any special permission.

The Declaration of Research and Publication Ethics

The authors of the paper declare that they comply with the scientific, ethical and quotation rules of SAUJS in all processes of the paper and that they do not make any falsification on the data collected. In addition, they declare that Sakarya University Journal of Science and its editorial board have no responsibility for any ethical violations that may be encountered, and that this study has not been evaluated in any academic publication environment other than Sakarya University Journal of Science.

REFERENCES

[1] S.P. Kodal and Z. Aksu, "Cationic surfactant-modified biosorption of anionic dyes by dried Rhizopus arrhizus." Environmental technology, vol. 38, no. 20, pp. 2551-2561, 2017.

[2] Z. Aksu, “Application of biosorption for the removal of organic pollutants: a review.” Process Biochemistry, vol. 40, pp. 997−1026, 2005.

[3] E. Bayram and E. Ayranci, “Investigation of changes in properties of activated carbon cloth upon polarization and of electrosorption of the dye basic blue-7.” Carbon, vol. 48, pp. 1718–1730, 2010.

[4] S.P.D Monte Blanco, F.B. Scheufele, A.N. Modenes, F.R. Espinoza-Quinones, P. Marin, A.D. Kroumov and C.E. Borba, “Kinetic, equilibrium and thermodynamic phenomenological modeling of reactive dye adsorption onto polymeric adsorbent.” Chemical Engineering Journal, vol. 307, pp. 466-475, 2017.

[5] Z. Aksu and A. İsoglu, “Use of agricultural waste sugar beet pulp for the removal of Gemazol turquoise blue-G reactive dye from aqueous solution.” Journal of Hazardous Materials B, vol. 137, pp. 418-430, 2006.

[6] A.A. Attia, B.S. Girgis, and N.A. Fathy, “Removal of methylene blue by carbons derived from peach stones by H_3PO_4 activation: batch and column studies.” Dyes and Pigments, vol. 76, pp. 282–289, 2008.

[7] M, Olivares-Marín, C. Fernández-González A. Macías-García, and V. Gómez-Serrano,

"Preparation of activated carbons from cherry stones by activation with potassium hydroxide." Applied Surface Science, vol. 252,pp. 5980–5983, 2006.

[8] W. Li, K. Yang, J. Peng, L. Zhang, S. Guo, and H. Xia, "Effects of carbonization temperatures on characteristics of porosity in coconut shell chars and activated carbons derived from carbonized coconut shell chars." Industrial Crops and Products, vol. 28, pp. 190–198, 2008.

[9] I.A.W. Tan, A.L. Ahmad, and B.H. Hameed, "Adsorption of basic dye on high-surface-area activated carbon prepared from coconut husk: equilibrium, kinetic and thermodynamic studies." Journal of Hazardous Materials, vol. 154, pp. 337–346, 2008.

[10] F.S. Vieira, A.R. Cestari, I.F. Gimenez, N.L.V. Carreño, and L.S. Barreto, "Kinetic and calorimetric study of the adsorption of dyes on mesoporous activated carbon prepared from coconut coir dust."Journal of Colloid and Interface Science, vol. 298, pp. 515–522, 2006.

[11] M. Olivares-Marín, V. Del-Prete, E. Garcia-Moruno, C. Fernández-González, A. Macías-García, and V. Gómez-Serrano, "The development of 500 an activated carbon from cherry stones and its use in the removal of ochratoxin A from red wine." Food Control. vol. 20, no. 3, pp. 298–303,2009.

[12] J.M. Dias, M.C.M. Alvim-Ferraz, M.F. Almeida, J. Rivera-Utrilla, and M. Sánchez-Polo. "Waste materials for activated carbon preparation and its use in aqueous-phase treatment: a review." Journal of Environmental Management, vol. 85, no. 4, pp. 833–846, 2007.

[13] S. Liang, X. Guo, N. Feng, and Q. Tian "Application of orange peel xanthate for the adsorption of Pb^{2+} from aqueous solutions." Journal of Hazardous Materials, vol. 170, pp. 425-429, 2010.

[14] D.D. Lu, Q.L. Cao, X.M. Li, X. Cao, F. Luo, and W. Shao, "Kinetics and equilibrium of Cu(II) adsorption onto chemically modified orange peel cellulose biosorbents." Hydrometallurgy, vol. 95, no. 1-2, pp. 145-152, 2009.

[15] P.D. Pathak, S.A. Mandavgane, and B.D. Kulkarni, "Characterizing fruit and vegetable peels as bioadsorbents." Current Science, vol. 110, pp. 2114–2123, 2016.

[16] J.J.M Órfão, A.I.M. Silva, J.C.V. Pereira, S. A. Barata, I. M. Fonseca, P. C. C. Faria, and M. F. R. Pereira. "Adsorption of a reactive dye on chemically modified activated carbons–influence of pH." Journal of Colloid and Interface Science, vol. 296, no. 2, pp. 480–489, 2006.

[17] N.H. Tran, S.J. You, and H.P. Chao, "Thermodynamic parameters of cadmium adsorption onto orange peel calculated from various methods: A comparison study." Journal of Environmental Chemical Engineering, vol. 4, pp. 2671–2682, 2016.

[18] I. Langmuir, "The adsorption of gases on plane surfaces of glass, mica, and platinum." Journal of the American Chemical Society, vol. 40, pp. 1361–140, 1918.

[19] Z. Aksu, A.I Tatlı, and Ö. Tunç, "A comparative adsorption/biosorption study of Acid Blue 161: Effect of temperature on equilibrium and kinetic parameters." Chemical Engineering Journal, vol. 142, pp. 23-39, 2008.

[20] Q. Meng, Q. Kaiqiang, M. Liying, H. Chunnian, L. Enzuo, H. Fang, S. Chunsheng, L. Qunying, L. Jiajun, and Z. Naiqin, "N-doped porous carbon nanofibers/porous silver network hybrid for high-rate supercapacitor electrode." ACS applied materials & interfaces, vol. 9, no. 36, pp. 30832-30839, 2017.

[21] Karaman C., Bayram E., Karaman O., Aktaş Z., "Preparation of high surface area nitrogen doped graphene for the assessment of

morphologic properties and nitrogen content impacts on supercapacitors", JOURNAL OF ELECTROANALYTICAL CHEMISTRY, vol.868, pp.114197-, 2020

[22] E. Errais, J. Duplay, M. Elhabiri, M. Khodja, R. Ocampo, R. Baltenweck-Guyot, and F. Darragi "Anionic RR120 dye adsorption onto raw clay: surface properties and adsorption mechanism." Colloids and Surfaces A: Physicochemical and Engineering Aspects, vol. 403, 69–78, 2012.

[23] J. Huang, D. Liu, J. Lu, H. Wang, X.Wei, and J. Liu "Biosorption of reactive black 5 by modified *Aspergillus versicolor* biomass: kinetics, capacity and mechanism studies." Colloids and Surfaces A: Physicochemical and Engineering Aspects, vol. 492, pp. 242–248, 2016.

[24] A. Srinivasan, and T. Viraraghavan, "Decolorization of dye wastewaters by biosorbents: a review." Journal of Environmental Management, vol. 91, pp. 1915–1929, 2010.

[25] Y.S. Al-Degs, M.I. El-Barghouthi, A.H. El-Sheikh, and G.M. Walker, "Effect of solution pH, ionic strength, and temperature on adsorption behavior of reactive dyes on activated carbon." Dyes and Pigments, vol. 77, pp.16–23, 2008.

[26] A.R. Cestari, E.F.S. Vieira, A.G.P. Dos Santos, J.A. Mota, and V.P. De Almeida, "Adsorption of anionic dyes on chitosan beads. 1. The influence of the chemical structures of dyes and temperature on the adsorption kinetics." Journal of Colloid and Interface Science, 280, 380–386, 2004.

Appendices

Molecular Structure of RBB

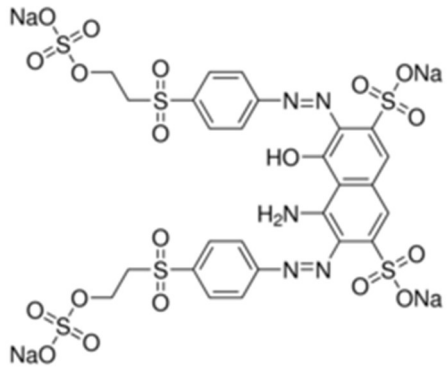

Figure 1 The Structural molecular formula of RBB [1]

Details for kinetic modelling of adsorption

In order to evaluate the adsorption kinetics, three simplified kinetic models including were applied to the experimental data: pseudo-first-order, pseudo-second-order, and saturation type. The related equations are given on Table A1. Principally, all of these three kinetic models include all of the mass transfer steps of the adsorption process, so they are called as pseudo-models.

Table A1
Simplified adsorption kinetic models

Kinetic Model	*Non-Linear Function*	*Linearized Function*
Pseudo-first order	$\frac{dq}{dt} = k_{1.ad}\,(q_{eq} - q)$	$\log(q_{eq} - q) = \log(q_{eq}) - \frac{k_{1.ad}}{2.303}t$
Pseudo-second order	$\frac{dq}{dt} = k_{2.ad}\,(q_{eq} - q)^2$	$\frac{t}{q} = \frac{1}{k_{2.ad}q_{eq}^2} + \frac{1}{q_{eq}}t$
Saturation type	$r_{ad} = \frac{dq}{dt}\Big\vert_{t=0} = \frac{k_{ad}\,C_0}{1 + k_{0.ad}\,C_0}$	$\frac{1}{r_{ad}} = \frac{1}{k_{ad}\,C_0} + \frac{k_{0.ad}}{k_{ad}}$

$k_{1,ad}$ *(min^{-1});* $k_{2,ad}$ *(g.mg^{-1}min^{-1});* k_{ad} *(L.g^{-1}min^{-1}) and* $k_{0,ad}$ *(L.mg^{-1})* are the of pseudo-first order, pseudo-second order and saturation type adsorption rate constants, respectively; r_{ad} is the initial adsorption rate at $t=0$; q_{eq} is the amount of adsorbed dye per gram of adsorbent at equilibrium ($mg.g^{-1}$).

Details for kinetic and equilibrium modelling of adsorption

To discover the maximum RBB adsorption capacity of the adsorbents, the experimental data were fitted to the Freudlich and Langmuir models which are most commonly used adsorption isotherms characterizing the non-linear equilibrium between adsorbed effluent on the active sites of the adsorbent (q_{eq}) and effluent in the bulk solution (C_{eq}) at a constant temperature, represented in Table A2.

Tabel A2
Adsorption isotherm models

Isotherm Model	*Equation*	*Nomenclature*
Langmuir Model	$q_{eq} = \frac{Q^o\,b\,C_{eq}}{1 + b\,C_{eq}}$	$\mathbf{Q^o}$; The maximum adsorption capacity $\boldsymbol{b}$; Bonding energy of adsorption $\boldsymbol{C_{eq}}$; Residual dye concentration at equilibrium ($mg.\,L^{-1}$)
Freundlich Model	$q_{eq} = K_F C_{eq}^{1/n}$	$\boldsymbol{K_F}$; Freundlich adsorption constant about adsorption capacity [$(mg.g^{-1}).(mg.L^{-1})^n$] $\boldsymbol{n}$; Freundlich adsorption constant (about adsorption intensity)